

## CHANGES IN THE MICROSTRUCTURE OF Fe-DOPED $\text{Gd}_5\text{Si}_2\text{Ge}_2$

### SPREMEMBE V MIKROSTRUKTURI ZLITINE $\text{Gd}_5\text{Si}_2\text{Ge}_2$ , DOPIRANE Z Fe

Irena Škulj<sup>1</sup>, Paul McGuiness<sup>2</sup>, Benjamin Podmiljšak<sup>2</sup>

<sup>1</sup>Institute of Metals and Technology, Ljubljana, Lepi pot 11, 1000 Ljubljana, Slovenia

<sup>2</sup>Jožef Stefan Institute, Jamova 39, 1000 Ljubljana, Slovenia  
irena.skulj@imt.si

Prejem rokopisa – received: 2008-01-03; sprejem za objavo – accepted for publication: 2008-03-25

$\text{Gd}_5\text{Si}_2\text{Ge}_2$ -based alloys can exhibit a giant magnetocaloric effect (MCE); this gives them the potential for use in cooling and refrigeration technologies. Cast alloys of this type have been reported to exhibit a three-phase microstructure: the main phase has a composition close to  $\text{Gd}_5(\text{Si}_{1.95}\text{Ge}_{2.05})$ ; the secondary phases are  $\text{Gd}_1(\text{Si},\text{Ge})_1$  and  $\text{Gd}_5(\text{Si},\text{Ge})_3$ , with the latter reported to have linear features in the microstructure, characteristic of a Widmanstätten pattern. In this investigation we have looked at the effect on the microstructure of  $\text{Gd}_5\text{Si}_2\text{Ge}_2$  resulting from a substitution of Si by Fe, according to the formula  $\text{Gd}_5\text{Si}_{2-x}\text{Fe}_x\text{Ge}_2$ , where  $x$  was varied between 0 and 1. Alloys with six different compositions were prepared using the arc-melting technique. All the samples and their microstructures were observed examined in optical microscope (OM) and a field-emission-gun scanning electron microscope (FEG SEM). The microstructures were quantitatively assessed with energy-dispersive X-ray spectroscopy (EDS) and the samples were characterised using X-ray diffraction (XRD).

Keywords: magnetocaloric effect, microstructure,  $\text{Gd}_5\text{Si}_2\text{Ge}_2$ -type alloys

Zlitine  $\text{Gd}_5\text{Si}_2\text{Ge}_2$  imajo dobre magneto-kalorične lastnosti (MCE) in so zaradi tega potencialno uporabne v hladilni in zmrzovalni tehnologiji. Lite mikrostrukture teh zlitin imajo večfazno strukturo, in sicer jo sestavljajo glavna faza s sestavo blizu  $\text{Gd}_5(\text{Si}_{1.95}\text{Ge}_{2.05})$  in dve sekundarni fazi  $\text{Gd}_1(\text{Si},\text{Ge})_1$  in  $\text{Gd}_5(\text{Si},\text{Ge})_3$ . V mikrostrukturi je opaziti fazo podolgovate oblike, ki jo lahko označimo kot Widmanstättenov vzorec. V delu teh raziskav smo se posvetili raziskavam sprememb mikrostrukture zlitine  $\text{Gd}_5\text{Si}_2\text{Ge}_2$ , ko v sestavi Si nadomeščamo z Fe. Sestave vzorcev ustrezajo  $\text{Gd}_5\text{Si}_{2-x}\text{Fe}_x\text{Ge}_2$ , kjer smo vzeli vrednosti  $x$  med 0 in 1. Zlitine vseh šestih različnih sestav smo pripravili z obločnim taljenjem. Njihove mikrostrukture smo pregledali v optičnem mikroskopu (OM) in vrstičnim elektronskim mikroskopu na poljsko emisijo (FEG SEM). Mikrostrukture smo kvantitativno analizirali z energijsko disperzivnim spektrometrom (EDS) in faze identificirali z rentgensko spektrometrijo (XRD).

Ključne besede: magneto-kalorimetrija, mikrostruktura, zlitine  $\text{Gd}_5\text{Si}_2\text{Ge}_2$

## 1 INTRODUCTION

The discovery of  $\text{Gd}(\text{Si},\text{Ge}_{1-x})_4$  alloys goes back to the late 1960s<sup>1,2</sup>.  $\text{Gd}_5\text{Si}_4$  orders ferromagnetically at  $T_c = 335$  K, and as much as 50 % of the Si can be substituted while maintaining the magnetic properties and the orthorhombic structure. Percharsky and Gschneidner<sup>3</sup> were, however, the first to report a large, near-room-temperature magnetocaloric effect (MCE) in these alloys.

$\text{Gd}_5\text{Si}_2\text{Ge}_2$ -type alloys with a monoclinic structure at room temperature all exhibit the giant magnetocaloric effect, from 46 J/(kg K) at 195 K to 16 J/(kg K) at 310 K<sup>4</sup>. The temperature at which the large magnetocaloric effect is observed can be easily adjusted between  $\approx 190$  K and 300 K by varying the chemical composition, i.e., by varying the Si/Ge ratio between 0.6 and 1.1.

Reversible first-order transitions from ferromagnetic to paramagnetic (FM $\leftrightarrow$ PM) for  $\text{Gd}_5(\text{Si},\text{Ge}_{1-x})_4$  where  $0.37 \leq x \leq 0.52$  can be induced by either temperature or magnetic field<sup>5</sup>. The co-existence of both FM and PM phases indicates the formation of a heterogeneous system with magnetically ordered and magnetically

disordered phases. The application of a magnetic field to the PM regions restores the FM phase by shifting the  $T_c$ .

These alloys form  $\text{Gd}_5\text{Si}_2\text{Ge}_2$ -type columnar cellular grains as the matrix phase and some additional phases located along the grain boundaries<sup>6</sup>. The additional phases are known as the  $\text{GdGe}$ - and  $\text{GdSi}_{2-x}$ -type phases. The room-temperature matrix monoclinic phase transforms into the orthorhombic  $\text{Gd}_5\text{Si}_4$ -type phase during cooling, without any apparent microstructural changes.

At low temperatures  $\text{Gd}_5(\text{Ge}_{1-x}\text{Si}_x)_4$  adopts an orthorhombic  $\text{Gd}_5\text{Si}_4$ -type structure, and the ground state is ferromagnetic<sup>7</sup>. At room temperature three different structures were observed, depending on the composition. For  $x > 0.55$  the  $\text{Gd}_5\text{Si}_4$  structure is stable, for  $x < 0.3$  the  $\text{Sm}_5\text{Ge}_4$ -type structure was observed, and for  $0.3 < x < 0.55$  the  $\text{Gd}_5\text{Si}_2\text{Ge}_2$ -type structure with an intermediate volume is formed. These three structures types are closely related. All three unit cells contain four formula units and essentially only differ in the mutual arrangement of identical building blocks, which are either connected by two, one or no covalent-like Si-Ge bonds, resulting in successively increasing unit-cell volumes<sup>7,8</sup>.

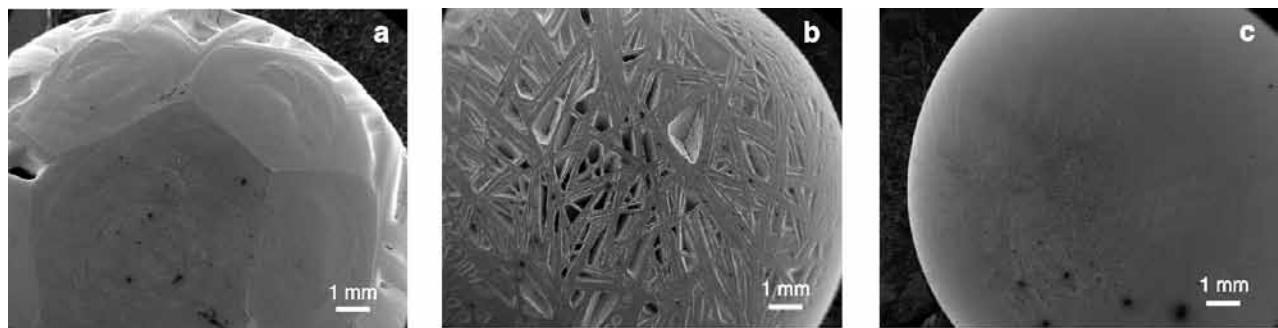


**Figure 1:** SEI taken of arc-melted buttons with G<sub>0</sub> (a), G<sub>2</sub> (b) and G<sub>4</sub> (c) compositions  
**Slika 1:** SEM-posnetki obločnotaljenih vzorcev s sestavami G<sub>0</sub> (a), G<sub>2</sub> (b) in G<sub>4</sub> (c)

## 2 EXPERIMENTAL DETAILS

The compositions studied in this research were  $\text{Gd}_5\text{Si}_{2-x}\text{Fe}_x\text{Ge}_2$  with  $x = 0, 0.125, 0.25, 0.5, 0.75$  and 1. All the compositions of the samples are collected in **Table 1**, together with the respective sample codes, G<sub>0</sub>, G<sub>05</sub>, G<sub>1</sub>, G<sub>2</sub>, G<sub>3</sub>, and G<sub>4</sub>. All the samples were prepared from high-purity starting elements with the mass fractions of gadolinium (99.99 %), silicon (99.995 %), germanium (99.999 %) and iron (99.99 %). The samples were prepared by arc-melting a mixture of pure elements on a water-cooled copper hearth in an argon atmosphere with a pressure of 0.5 bar. Each sample was re-melted three times and after each re-melting the samples were turned over to ensure their homogeneity. All the samples were prepared as 5 g buttons.

**Table 1:** The compositions of all alloys used in this work in the mole fractions (%)

**Tabela 1:** Sestave vzorcev, uporabljenih v raziskovalnem delu v molskih deležih (%)

	Gd	Si	Fe	Ge
G <sub>0</sub>	55.6	22.2	/	22.2
G <sub>05</sub>	55.6	20.8	1.4	22.2
G <sub>1</sub>	55.6	19.4	2.8	22.2
G <sub>2</sub>	55.6	16.6	5.6	22.2
G <sub>3</sub>	55.6	13.9	8.3	22.2
G <sub>4</sub>	55.6	11.1	11.1	22.2

All the samples were cut and cross-sectioned, and then polished for the optical and electron microscopy. All the microstructures were inspected with an optical microscope and quantitatively assessed with a FEG SEM, with all the phases analysed with EDS. All the XRD patterns for all the samples were collected using Cu-K $\alpha$  radiation.

## 3 RESULTS

### 3.1 Microstructure

The electron microscopy SE images in **Figure 1** show the macrostructures of three of the arc-melted buttons. The differences in the upper surfaces of the button sample are strikingly different. The G<sub>0</sub> sample

exhibits regular pentagons and hexagons reminiscent of a buckyball. The G<sub>2</sub> sample's surface shows a sinew effect, rather like columnar grains running at angles on the upper surface of the sample. The G<sub>4</sub> sample has a smooth upper surface, much more characteristic of an intermetallic arc-melted button.

Optical micrographs taken of the set of  $\text{Gd}_5\text{Si}_{2-x}\text{Fe}_x\text{Ge}_2$  samples with  $x = 0, 0.125, 0.25, 0.5, 0.75$  and 1 are shown in **Figure 2**. It is clear from the six images that all the samples consist of multi-phase structures. The microstructure of the G<sub>0</sub> sample, where  $x = 0$ , consists of the  $\text{Gd}_5(\text{Si},\text{Ge})_4$  matrix phase A and a grain-boundary phase. A new matrix phase, the B phase, appears with the smallest addition of iron, i.e., the G<sub>05</sub> sample. The composition of the matrix phase B suggest that it is a  $\text{Gd}_5(\text{Si},\text{Ge})_3$ -type phase. With increasing

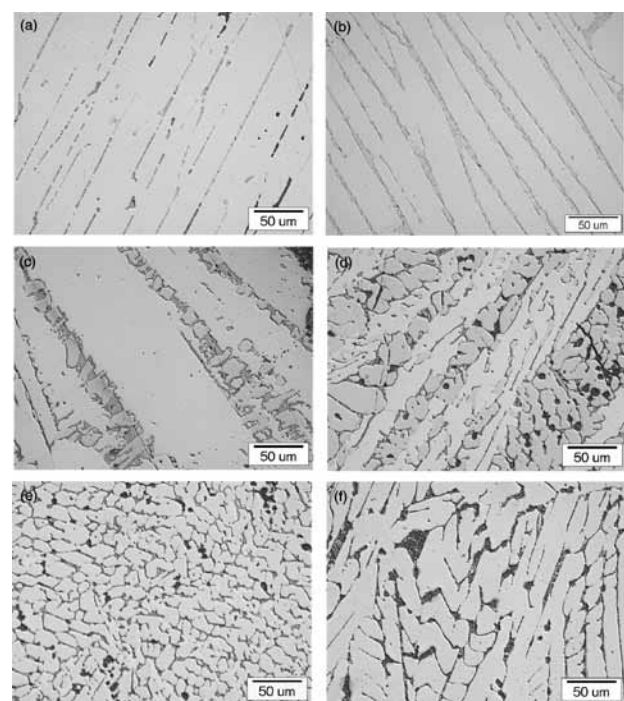


**Figure 2:** Optical images of the etched microstructures of arc-melted G<sub>0</sub> (a), G<sub>05</sub> (b), G<sub>1</sub> (c), G<sub>2</sub> (d), G<sub>3</sub> (e) and G<sub>4</sub> (f) samples

**Slika 2:** Optični posnetki jedkanih mikrostruktur obločnotaljenih vzorcev G<sub>0</sub> (a), G<sub>05</sub> (b), G<sub>1</sub> (c), G<sub>2</sub> (d), G<sub>3</sub> (e) in G<sub>4</sub> (f)

amounts of added iron the amount of matrix phase A is seen to decrease until it disappears completely in sample  $G_4$ , the point where half of silicon is replaced by iron. It is also worth noting that approximately half of the matrix phase A is replaced by matrix phase B in the  $G_2$  sample with  $x = 0.5$ .

### 3.2 Phase compositional analyses

The compositions of the matrix phases A and B with respect to the amount of added iron can be seen in **Table 2**. The compositions strongly suggest that matrix phase A is a  $\text{Gd}_5\text{Si}_4$ -type phase, while matrix phase B is better described by the composition  $\text{Gd}_5\text{Si}_3$ . The amount of the dissolved Fe in both of the matrix phases increases with the increasing amount of added iron; however, there is some variability in the analyses. This is particularly so for the amount of Fe dissolved in matrix phase B. It should be noted, however, that the amounts of iron in the matrix phases are very low; in all cases the mole fraction is  $<1.5\%$ .

The compositions of the grain-boundary phases analysed for all six samples are collected in **Table 3**. Three different grain-boundary phases were identified. The grain-boundary phase found in sample  $G_0$  is not significantly different from that of the matrix phase, and this phase is only present in this sample, the one with no iron in the initial composition. The grain-boundary phase GB2 appears in all the samples with any amount of iron present in the initial composition. The composition of this GB2 phase does not vary with increasing amounts of

added Fe, and the ratio for  $\text{Gd:Si:Fe}$  is approximately 1:1:1. The grain-boundary phase GB3 starts forming in the structure of the samples as a grain-boundary phase when  $x$  becomes larger than 0.5, i.e., in samples  $G_3$  and  $G_4$ . The composition of the GB3 phase was different for the two samples, but in this case the values of the mole fractions are very high, i.e.,  $>50\%$ .

### 3.3 XRD

The XRD patterns of the as-arc-melted button samples can be seen in **Figure 3**. The peaks in the pattern that belongs to the  $G_0$  sample confirm that the main phase seen in the microstructure (**Figure 2a**) is the  $\text{Gd}_5\text{Si}_2\text{Ge}_2$  monoclinic phase. The vast majority of the

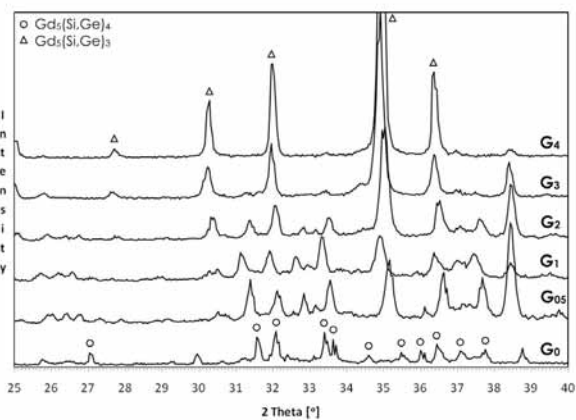


**Figure 3:** XRD patterns of arc-melted samples

**Slika 3:** Rentgenski spektri obločnotaljenih vzorcev

**Table 2:** Elemental compositions in mole fractions (%) of the two main phases present in the samples evaluated using EDS. Analysing errors to be considered are  $\text{Gd} \pm 0.2$ ,  $\text{Si} \pm 0.1$ ,  $\text{Fe} \pm 0.2$  and  $\text{Ge} \pm 0.3$ .

**Tabela 2:** Elementarne sestave v molskih deležih (%) obeh glavnih faz v mikrostrukturah, pridobljenih z EDS. Napake pri analizah so:  $\text{Gd} \pm 0.2$ ,  $\text{Si} \pm 0.1$ ,  $\text{Fe} \pm 0.2$  in  $\text{Ge} \pm 0.3$

	Phase A				Phase B			
	Gd	Si	Fe	Ge	Gd	Si	Fe	Ge
$G_0$	55.8	23.7	/	20.5			—	
$G_{05}$	55.2	20.7	0.5	23.6	61.5	16.1	0.6	21.8
$G_1$	56.2	20.0	0.5	23.3	62.8	16.2	1.0	20.6
$G_2$	56.2	17.6	0.8	25.4	63.2	13.8	0.6	22.4
$G_3$	56.3	15.2	0.7	27.8	61.8	11.1	0.7	26.4
$G_4$		—			61.8	11.7	1.3	25.2

**Table 3:** Elemental compositions in mole fractions (%) of the grain-boundary phases present in the samples evaluated using EDS. Analysing errors to be considered are  $\text{Gd} \pm 0.2$ ,  $\text{Si} \pm 0.1$ ,  $\text{Fe} \pm 0.2$  and  $\text{Ge} \pm 0.3$ .

**Tabela 3:** Elementarne sestave v molskih deležih (%) faz na mejah med kristalnimi zrni glavnih faz, pridobljenih z EDS. Napake pri analizah so:  $\text{Gd} \pm 0.2$ ,  $\text{Si} \pm 0.1$ ,  $\text{Fe} \pm 0.2$  in  $\text{Ge} \pm 0.3$

	GB phase 1				GB phase 2				GB phase 3			
	Gd	Si	Fe	Ge	Gd	Si	Fe	Ge	Gd	Si	Fe	Ge
$G_0$	51.5	31.7	/	17.0			—				—	
$G_{05}$		—			34.8	27.4	33.3	4.5			—	
$G_1$		—			35.5	28.0	30.8	5.6			—	
$G_2$		—			35.5	26.9	31.7	5.9			—	
$G_3$		—			35.3	26.3	31.4	7.0	33.1	5.5	59.9	1.5
$G_4$		—			33.2	28.3	34.5	4.0	31.3	13.2	53.1	2.5

peaks agree with the calculated pattern for the  $\text{Gd}_5\text{Si}_2\text{Ge}_2$  compound. The positions of the calculated peaks are identified by the circles in **Figure 3**. New peaks can be observed in the other patterns as a result of the formation of new phases in all the samples with added iron, i.e., where  $x \neq 0$ . Some shifts in the peaks, while maintaining the same structure, can also be seen, and these shifts result from the iron entering both A and B matrix phases and forming solid solutions. The pattern of the  $\text{G}_4$  sample indicates that the matrix phase B is the only matrix phase still present in the sample.

#### 4 DISCUSSION

The unusual macrostructural features observed for the samples with no iron and very small amounts of iron are very striking; however, during our microstructural investigations on cross-sections near the surface, these features were found to penetrate only short distances into the sample, and in no way were they representative of the bulk. The formations – the buckyballs and the sinews – are clearly related to the cooling rate, which is very fast in such a system, but very small amounts of iron are clearly the decisive factor. The very high aspect ratios of the sinews are indicative of strongly anisotropic grain grown on the sample's surface, which must be a consequence of the dissolved iron, whereas the buckyballs point to a surface-energy effect, with the flat surfaces representing the growth of particular atomic planes. The smooth surface of the  $\text{G}_4$  sample implies that minimising surface area during the molten phase is still the predominant factor in determining the final shape of the solid button.

The optical micrographs in **Figure 3** show the gradual changes with compositional variations. The second matrix phase, B, begins to form between the grains of the original matrix phase, A, and then gradually comes to dominate the microstructure as the amount of iron in the sample increases. The EDS measurements clearly reveal the presence of iron in both matrixes A and B. However, the amount in the mass fractions of iron does not vary much, being between 0.5 % and 1.3 % for both phases in all the samples. Much more dramatic changes are seen in the amounts of Si and Ge in the matrix phases. In both cases the addition of iron at the

expense of Si causes Ge to substitute for the Si: in the  $\text{G}_5$  sample, for example, the relative amounts of Si and Ge in the two phases, A and B, were 20.7 : 23.6 and 16.1 : 21.8 respectively. By the time we reach sample  $\text{G}_3$ , the ratios have shifted to samples that are much richer in Ge, i.e. 15.2 : 27.8 and 11.1 : 26.4.

The XRD diffraction results are very clear in the case of the two matrix phases. The gradual disappearance of the  $\text{Gd}_5\text{Si}_2\text{Ge}_2$  phase as the iron is added, and the parallel growth of the  $\text{Gd}_5(\text{Si},\text{Ge})_3$  phase are easily seen. Unfortunately, however, the XRD data does not give us any help when trying to obtain structural information on the grain-boundary phases.

#### 5 CONCLUSIONS

It can be concluded that the  $\text{Gd}_5\text{Si}_{(2-x)}\text{Fe}_x\text{Ge}_2$  alloys where  $x$  varies between 0 and 1 show significant differences in both macrostructures and microstructures. The A matrix phase with the  $\text{Gd}_5(\text{Si},\text{Ge})_4$  composition when  $x = 0$  becomes the B matrix phase with the  $\text{Gd}_5(\text{Si},\text{Ge})_3$  composition when  $x = 1$ . All the samples with  $x$  between 0 and 1 show the presence of both matrix phases in the alloy. The substituted iron was found in all the matrix and grain-boundary phase, although the amounts in the matrix phases were very low. The iron contributes mainly to the grain-boundary phases that are formed and to a change in the relative amounts of Si and Ge in the matrix phases.

#### 6 REFERENCES

- <sup>1</sup>F. Holtzberg, R. J. Gambino, T. R. McGuire, *J. Phys. Chem. Solids*, 28 (**1967**), 2238
- <sup>2</sup>G. S. Smith, A. G. Tharp, Q. Johnson, *Acta Crystallogr.*, 22 (**1967**), 940
- <sup>3</sup>V. K. Pecharsky, K. A. Gschneider Jr.: *Phys. Rev. Lett.*, 78 (**1997**), 4494
- <sup>4</sup>A. O. Pecharsky, K. A. Gschneider Jr., V. K. Pecharsky, *JMMM*, 267 (**2003**), 60
- <sup>5</sup>E. M. Levin, K. A. Gschneider Jr., V. K. Pecharsky, *JMMM*, 231 (**2001**), 135
- <sup>6</sup>H. Fu, Y. Chen, M. Tu, T. Zhang, *Acta Materialia*, 53 (**2005**), 2377
- <sup>7</sup>A. O. Percharsky, K. A. Gschneider, V. K. Percharsky, C. E. Schindler, *J. Alloys Compounds*, 338 (**2002**), 126
- <sup>8</sup>Y. Mozharivskyj, A. O. Percharsky, V. K. Percharsky, G. J. Miller, *J. Am. Chem. Soc.*, 127 (**2005**), 317